Exceptional Negative Thermal Expansion in $AlPO_4$-17

Martin P. Attfield and Arthur W. Sleight*

Department of Chemistry and Center for Advanced Materials Research, Oregon State University, Corvallis, Oregon 97331-4003

Received March 12, 1998. Revised Manuscript Received May 11, 1998

Anhydrous $AlPO_4$-17 has been found to experience a very strong negative thermal expansion over the temperature range 18−300 K. Powder synchrotron X-ray diffraction data taken at six temperatures over this range show an essentially linear decrease in cell volume, with a linear coefficient of thermal expansion of -11.7×10^{-6} K^{-1} which is significantly more negative than previously reported for any material. The contraction of the structure along the *a* and *b* cell edges is considerably greater than along the *c* edge of this hexagonal structure. Rietveld refinements of the framework as a function of temperature suggest that the negative thermal expansion is related to the harmonic transverse vibrations of bridging oxygen atoms, which lead to dynamic rocking of the essentially rigid tetrahedral building blocks of the structure.

Introduction

In open framework structures, the transverse thermal motion of oxygen in M−O−M linkages can give rise to negative thermal expansion.[1−6] A requirement for such unusual behavior by this mechanism is strong M−O bonds which themselves show negligible thermal expansion. The thermal motions of oxygens will be highly correlated, and this is conveniently described by viewing network structures as corner-sharing polyhedra with coupled rocking motions of these linked polyhedra.[2−7] The polyhedra of the network can all be tetrahedra, in which case, lacking interstitial ions, the formula must be MO_2 with all oxygens coordinated to two M^{4+} cations. Indeed, amorphous SiO_2 shows negative thermal expansion below room temperature.[1] Quartz, cristobalite, and tridymite all show weak negative thermal expansion behavior above 1000 °C.[8] We have recently shown that SiO_2 with the faujasite structure has strong negative thermal expansion ($\alpha = -4.2 \times 10^{-6}$ K^{-1}) over the measured temperature range of 25−573 K.[6]

The study of the thermal expansion properties of zeolite-type materials is complicated by the presence of nonframework water and cations. Both may provide a positive or negative contribution to the expansion of the zeolite and disguise the intrinsic nature of the framework thermal expansion. This is seen in the experimental data for the thermal expansion of Na-zeolite X.[9] Hence, the study of the thermal expansion properties of the framework of these materials is best performed on siliceous or aluminophosphate materials, both of which are easy to dehydrate and have neutral frameworks rendering them free of nonframework cations.

The aluminophosphate, $AlPO_4$-17,[10,11] is comprised of alternating, corner-sharing AlO_4 and PO_4 tetrahedra. The structure is analogous to that of the zeolite erionite and is built up from 4- and 6-rings that are linked to form sheets that contain 6-rings, cancrinite cages, and 12-rings (Figure 1a,b). The sheets are connected along the *c* direction to form columns of alternating cancrinite cages and hexagonal prisms, as shown in Figure 1b,c. The 6-rings are stacked in AABAAC sequence which results in a structure containing cavities entered into through an 8-ring window and containing a 12-ring at their center (Figure 1c).[12] The negative thermal expansion property of this material has been predicted from the results of computer simulations,[13] but its range and magnitude have not been determined experimentally as far as the authors are aware. In this work we report on the magnitude and mechanism of the negative thermal expansion properties of dehydrated, calcined $AlPO_4$-17, determined from synchrotron X-ray powder diffraction data.

Experimental Section

The synthesis of $AlPO_4$-17 was based on that described by Lohse et al.[14] using aluminum hydroxide instead of aluminum isopropoxide as the aluminum source. The reactants used were aluminum hydroxide (Aesar), phosphoric acid (Mallinckrodt, 85.7% w/w), cyclohexylamine (CHA) (Aldrich), and deion-

* Corresponding author: Fax: (541) 737-4407. E-mail: sleighta@chem.orst.edu.

(1) White, G. K. *Contemp.Phys.* **1993**, *34*, 193.
(2) Korthuis, V.; Khosrovani, N.; Sleight, A. W.; Roberts, N.; Dupree, R.; Warren, W. W., Jr. *Chem. Mater.* **1995**, *7*, 412.
(3) Khosrovani, N.; Sleight, A. W. *Inorg. Chem.* **1996**, *35*, 485.
(4) Evans, J. S. O.; Mary, T. A.; Sleight, A. W.; Vogt, T. *Science* **1996**, *272*, 90.
(5) Evans, J. S. O.; Mary, T. A.; Vogt, T.; Subramanian, M. A.; Sleight, A. W. *Chem. Mater.* **1996**, *8*, 2809.
(6) Attfield, M. P.; Sleight, A. W. *Chem. Commun.* **1998**, 601.
(7) Pryde, A. K. A.; Hammonds, K. D.; Dove, M. Y.; Heine, V.; Gale, J. D.; Warren, M. C. *J. Phys. Condens. Matter* **1996**, *8*, 1.
(8) Taylor, D. *Br. Ceram. Trans. J.* **1984**, *83*, 129.
(9) Couves, J. W.; Jones, R. H.; Parker, S. C.; Tschaufeser, P.; Catlow, C. R. A. *J. Phys.: Cond. Matter* **1993**, *5*, L329.
(10) Wilson, S. T.; Lok, B. M.; Messina, C. A.; Cannan, T. R.; Flanigen, E. M. *J. Am. Chem. Soc.* **1982**, *104*, 1146.
(11) Wilson, S. T.; Lok, B. M.; Messina, C. A.; Cannan, T. R.; Flanigen, E. M. *ACS Symp. Ser.* **1983**, *218*, 79.
(12) Gard, J. A.; Tait, J. M. *Adv. Chem. Ser.* **1971**, *101*, 230.
(13) Tschaufeser, P.; Parker, S. C. *J. Phys. Chem.* **1995**, *99*, 10600.
(14) Lohse, U.; Loffler, E.; Kosche, K. Janchen, J.; Parlitz, B. *Zeolites* **1993**, *13*, 549.

S0897-4756(98)00158-6 CCC: $15.00
Published on Web 06/23/1998

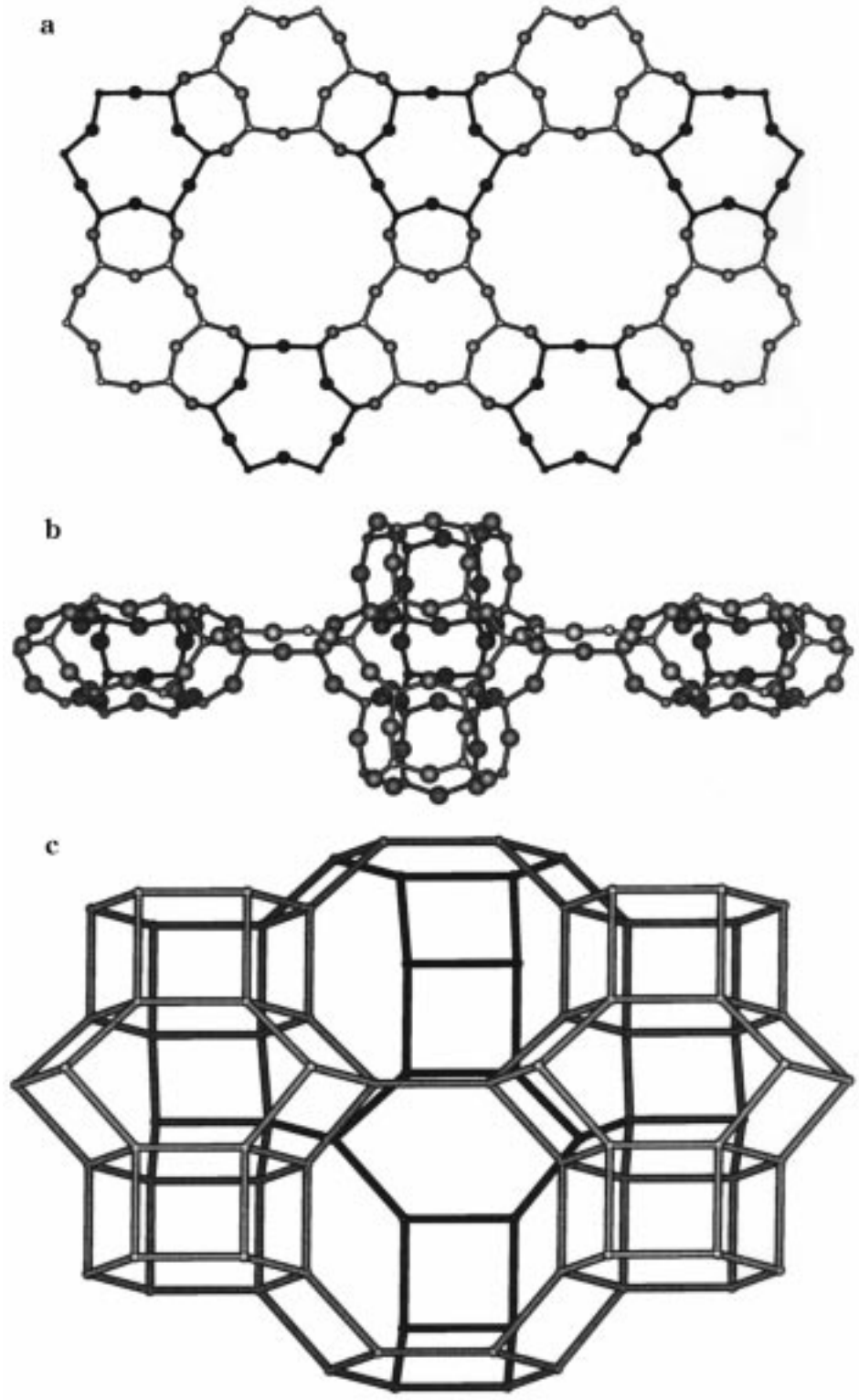

Figure 1. The structure of $AlPO_4$-17 (erionite): (a) a sheet of cancrinite cages and 6-rings viewed along the *c* axis; (b) the same sheet viewed along the *a* axis, with attached hexagonal prisms for the central cancrinite cage; and (c) the large cavity formed by stacking of the sheets. In panels a and b the larger spheres are the O atoms and the smaller ones are the Al or P atoms.

ized water. The oxide molar composition of the starting gel was Al_2O_3:P_2O_5:CHA:H_2O 1:1:1:50. The aluminum hydroxide and water were added to a 23 mL Teflon liner and stirred until a homogeneous suspension was formed. Phosphoric acid and CHA were then added slowly to the mixture, under intense stirring. The reaction mixture was sealed in a Parr digestion bomb and heated under hydrothermal autogenous conditions at 200 °C for 5 days. The white polycrystalline material was separated by suction filtration and shown to be a pure phase from its X-ray powder diffraction pattern. The sample was calcined under flowing oxygen at a temperature of 450 °C for 12 h to remove the CHA. TGA measurements on the resultant material showed that it lost approximately 20% of its weight by 100 °C, the weight loss was assumed to be due to the removal of adsorbed water.

The sample was dehydrated for 12 h at 200 °C under a vacuum of ~10−5 Torr and transferred to an argon filled glovebox where it was loaded and sealed into 0.5 and 0.3 mm diameter Lindemann glass capillary tubes. Synchrotron X-ray powder diffraction data were collected on the sample at

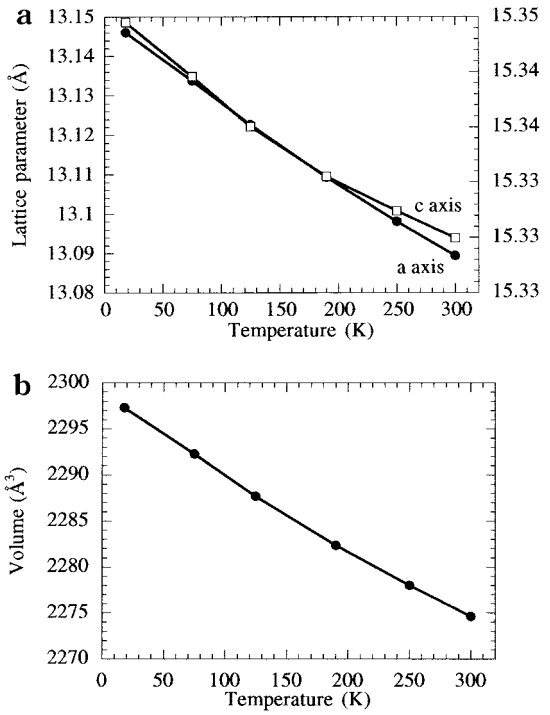

Figure 2. (a) Lattice parameters with *a* and *c* axis scales on left and right, respectively, and (b) unit cell volume as a function of temperature

beamline ×7A, National Synchrotron Light Source, Brookhaven National Laboratory. The diffractometer setup included the use of a Si(111) monochromator and a krypton-filled position-sensitive detector. All data were collected at an average wavelength of 1.09932(6) Å. The temperature of the sample for each data collection was controlled using an Air Products Displex, and data were collected at six temperatures between 18.00 and 300.00 K, inclusive. All structure refinements and calculations were performed within the GSAS suite of programs.[15] Further details of the refinements are given within the relevant sections.

Results

Negative Thermal Expansion Properties. The lattice parameters of $AlPO_4$-17 at each temperature were determined from a Le Bail profile fit[16] of the X-ray data set using the space group $P6_3/m$ (No. 176). This is the space group used to determine the crystal structure of as-synthesized $AlPO_4$-17.[17] The first seven highly asymmetrical peaks of the synchrotron X-ray data sets were excluded from the fit. The background for each data set was fit by linear interpolation using the same number of points in each case. The last cycle of least squares refinement included the zero point, lattice parameter, and four peak shape parameters. The X-ray data sets collected on the laboratory diffractometer were fit in a similar fashion. Only four asymmetric peaks were excluded from each refinement. The background was fit by linear interpolation and the last cycle of least squares refinement included the zero point, lattice parameters, and five peak shape parameters.

Figure 2 and Table 1 give the variation of the lattice parameters and unit cell volume as a function of temperature. An essentially linear decrease of *a* (-2.02×10^{-4} Å K^{-1}) and *c* (-6.94×10^{-5} Å K^{-1}) is seen over the entire temperature range; the decrease of *a* is much more marked than *c*. The overall volume contraction is well-represented by $V = -0.0807T + 2298.3$ and corresponds to a volume contraction coefficient $\alpha_V = -3.50 \times 10^{-5}$ K^{-1}. This gives a value of $\alpha_l = 1/3\alpha_V = -11.7 \times 10^{-6}$ K^{-1}, apparently the strongest negative thermal expansion reported for any material. The previous record holder was ZrW_2O_8 with $\alpha_l = -8.8 \times 10^{-6}$ K^{-1}.[4,5]

Table 1. Cell Dimensions as a Function of Temperature[a]

	Le Bail fits in $P6_3/m$			Rietveld fits in $P6_3/mmc$		
temp	*a* (Å)	*c* (Å)	*V* (Å^3)	χ^2	wR_p (%)	$R(F^2)$ (%)
18.00	13.14602(7)	15.34952(10)	2297.28(3)	1.591	3.40	7.15
75.00	13.13384(7)	15.34458(10)	2292.28(2)	1.443	3.32	6.77
125.00	13.12265(6)	15.34005(9)	2287.70(2)	1.391	3.16	6.81
190.00	13.10928(6)	15.33552(9)	2282.37(2)	1.437	3.18	7.28
250.00	13.09808(6)	15.33240(8)	2278.02(2)	1.296	3.16	6.98
300.00	13.08943(6)	15.32994(9)	2274.64(2)	1.338	3.28	6.31

[a] Values of χ^2, wR_p, and $R(F^2)$ are given for the Rietveld refinements of the structure in space group $P6_3/mmc$.

Table 2. Fractional Coordinates and Isotropic Temperature Factors for $AlPO_4$-17 at 300 K (space group $P6_3/m$)[a]

name	x	y	z	U_{iso} (Å^2)
P(1)	0.9978(7)	0.2383(6)	0.1012(4)	0.010(2)
P(2)	0.573(1)	0.909(1)	0.2500	0.014(3)
Al(1)	0.7633(7)	0.9990(9)	0.1009(5)	0.014(2)
Al(2)	0.094(1)	0.422(1)	0.2500	0.009(3)
O(1)	0.020(1)	0.345(1)	0.1575(6)	0.011(4)
O(1')	0.649(1)	0.965(1)	0.1685(6)	0.025(5)
O(2)	0.092(1)	0.2009(4)	0.1140(3)	0.020(2)
O(3)	0.133(2)	0.2544(4)	0.6261(3)	0.019(2)
O(4)	0.2774(9)	0.003(2)	1.005(1)	0.022(2)
O(5)	0.237(2)	0.4573(5)	0.2500	0.013(3)
O(6)	0.460(2)	0.9159(5)	0.2500	0.013(2)

[a] $a = 13.89787(7)$ Å, $c = 15.3302(1)$ Å, $V = 2274.80(3)$ Å, $\chi^2 = 1.270$, $wR_p = 3.18\%$, $R(F^2) = 6.89\%$.

Structure Refinements. The synchrotron X-ray data sets were used to refine the structure of $AlPO_4$-17 using the Rietveld method.[18] The refinement at each temperature was performed using the same procedure. The first seven peaks were excluded from each refinement due to their highly asymmetric peak shape. All backgrounds were fit by linear interpolation using the same number of points in each case. The starting model for the framework of $AlPO_4$-17 was taken from that described by Pluth and Smith[17] in space group $P6_3/m$, which allows for complete ordering of the Al and P atoms. The last cycle of least-squares refinement included the histogram scale factor, zero point, lattice parameter, four peak shape parameters, atomic coordinates, and the isotropic thermal parameter of each atom. The shifts of the atomic coordinates and thermal parameters at each temperature were damped to enable the refinement to converge. The final atomic coordinates and selected bond distances and angles of the structure at 300 K are given in Tables 2 and 3, respectively. The final observed, calculated, and difference plots are shown in Figure 3.

(15) Larson, A. C.; Von Dreele, A. B. GSAS, Technol. Rept. LA-UR-86−748; Los Alamos National Laboratory: Los Alamos, NM, 1987.
(16) Le Bail, A. C.; Duroy, H.; Fourquet, J. L. *Mater. Res. Bull.* **1988**, *23*, 447.
(17) Pluth, J. J.; Smith, J. V. *Acta Crystallogr. C*, **1986**, *42*, 283.
(18) Rietveld, H. M. *J. Appl. Crystallogr.* **1969**, *2*, 65.

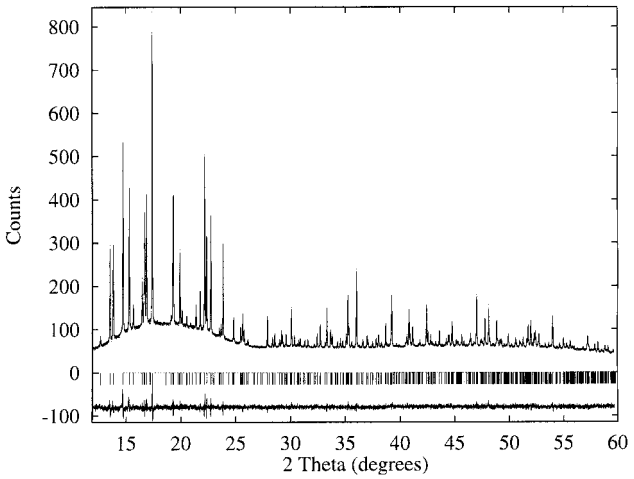

Figure 3. The final observed (dots), calculated (solid) and difference plot for the Rietveld refinement of dehydrated, calcined $AlPO_4$-17 at 300 K (space group $P6_3/m$).

Table 3. Selected Bond Distances (Å) and Angles (deg) in $AlPO_4$-17 at 300 K (space group $P6_3/m$)

P(1)−O(1)	1.55(1)	Al(1)−O(1')	1.69(1)
P(1)−O(2)	1.56(2)	Al(1)−O(2)	1.72(2)
P(1)−O(3)	1.53(2)	Al(1)−O(3)	1.70(2)
P(1)−O(4)	1.55(2)	Al(1)−O(4)	1.71(2)
mean P(1)−O	1.54	mean Al(1)−O	1.70
2 × P(2)−O(1')	1.54(1)	2 × Al(2)−O(1)	1.73(2)
P(2)−O(5)	1.54(3)	Al(1)−O(5)	1.70(3)
P(2)−O(6)	1.53(3)	Al(1)−O(6)	1.67(3)
mean P(2)−O	1.54	mean Al(2)−O	1.70
O(1)−P(1)−O(2)	113.4(7)	O(1')−Al(1)−O(2)	106.5(7)
O(1)−P(1)−O(3)	108.9(7)	O(1')−Al(1)−O(3)	110.4(7)
O(1)−P(1)−O(4)	106.3(6)	O(1')−Al(1)−O(4)	110.5(6)
O(2)−P(1)−O(3)	107.4(5)	O(2)−Al(1)−O(3)	111.1(6)
O(2)−P(1)−O(4)	110.2(7)	O(2)−Al(1)−O(4)	108.2(7)
O(3)−P(1)−O(4)	110.7(9)	O(3)−Al(1)−O(4)	110.1(8)
O(1')-P(2)−O(1'))	108.7(7)	O(1)−Al(2)−O(1)	110.1(11)
2 × O(1')-P(2)−O(5)	106.0(7)	2 × O(1)−Al(2)−O(5)	112.5(6)
2 × O(1')-P(2)−O(6)	112.8(7)	2 × O(1)−Al(2)−O(6)	105.7(5)
O(5)−P(2)−O(6)	110.0(7)	O(5)−Al(2)−O(6)	110.1(9)
P(1)−O(1)−Al(2)	141.7(8)	P(2)−O(1')−Al(1)	154.6(9)
P(1)−O(2)−Al(1)	147.1(4)	P(1)−O(3)−Al(1)	149.3(4)
P(1)−O(4)−Al(1)	144.2(3)	P(2)−O(5)−Al(2)	153.3(5)
P(2)−O(6)−Al(2)	173.2(5)		

The framework topology of dehydrated $AlPO_4$-17 matches that of erionite (see Figure 1), as expected, except for the strict alternation of Al and P over the tetrahedral nodes. In comparing this structure to that of the as-synthesized material described by Pluth and Smith,[17] we find no trace of any residual water or hydroxyl species present in the structure; as a result, the coordination of Al(1) is found to be that expected for a regular tetrahedral AlO_4 unit. All the bond distances and angles are reasonable for PO_4 and AlO_4 tetrahedra when compared to others found in the literature. For example, in the as-synthesized $AlPO_4$-17 structure,[16] the average Al−O and P−O bond lengths and O−Al−O and O−P−O tetrahedral angles are 1.520 Å, 1.718 Å, 109.3°, and 109.4°, respectively.

The refinement results of the structure at the lower temperatures gave the same framework structure. However, when comparing the values of the T−O bond distances (where T = tetrahedral atom, Al or P), internal O−T−O bond angles of the constituent tetrahedra, and the bridging T−O−T angles as a function of temperature, no clear trends could be determined. This is not too surprising when we consider the maximum overall change in bond distances we might expect to observe from 18 to 300 K (assumed to have the same relative change as the *a* cell parameter) would be 1.740−1.733 Å for an Al−O bond compared to the average Rietveld esd on a bond length in our refinements of 0.02 Å and considering that Rietveld esds are typically underestimated.

The large esds are indicative of the problem in determining ordered aluminophosphate framework structures from powder diffraction data. It is often found that there are too few well-resolved, independent reflections that can be used to accurately determine the structure with ordered Al and P atoms compared to the structure where Al and P atoms are randomly distributed over the same sites, even though the former is believed to be the chemically correct model. The most extreme case of this problem arises when both the space group for the ordered and disordered structure have the same systematic absences and the space group of the ordered structure imposes no restrictions on the phases of the reflections or the position of the origin. An example of this case is found in the precision of the structure refinements of calcined $AlPO_4$-11 from powder neutron diffraction data.[19]

If $AlPO_4$-17 is considered to have a disordered arrangement of Al and P atoms over the tetrahedral nodes, then the space group of the structure becomes $P6_3/mmc$ (No. 194). The (*hhl*) reflections are absent in this space group, which is not the case for these reflections in our diffraction data. However, only one, the (113) reflection, of the 29 (*hhl*) reflections in the 2θ range we are considering has a significant intensity and is well-resolved, which clearly makes it difficult to obtain the high precision structures needed to investigate the mechanism of negative thermal expansion for this material. Thus, we decided to refine the structure of $AlPO_4$-17 in space group $P6_3/mmc$ at each temperature. Even though this is not the correct space group, it allows a series of more precise structures to be obtained which may be used to explain the mechanism of negative thermal expansion in $AlPO_4$-17.

The starting model for the framework of $AlPO_4$-17 in space group $P6_3/mmc$ was taken from that described by Pluth and Smith in space group $P6_3/m$[17] with the appropriate reduction of the number of atomic sites for atoms that become equivalent and movement of atoms onto the special positions. Each of the two tetrahedral sites was considered to be half-occupied by P and Al atoms. The (113) reflection was excluded from each of the refinements. The last cycle of least squares refinement included the histogram scale factor, zero point, lattice parameter, four peak shape parameters, atomic coordinates, and two thermal parameters. The thermal parameters of all the Al and P atoms were constrained to have the same value, and oxygen atoms were all constrained to have the same thermal parameters. The final atomic coordinates of the structures at 18 and 300 K are given in Table 4 and selected bond distances and angles of the structure at 300 K are given in Table 5.

(19) Richardson, J. W., Jr.; Pluth, J. M.; Smith, J. V. *Acta Crystallogr. B* **1988**, *44*, 367.

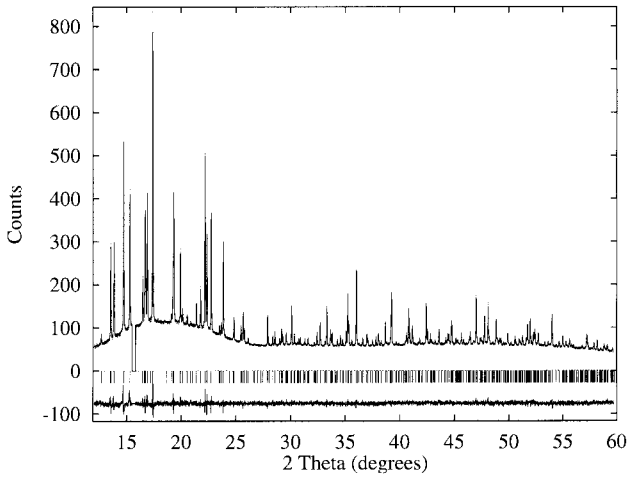

Figure 4. The final observed (dots), calculated (solid) and difference plot for the Rietveld refinement of dehydrated, calcined $AlPO_4$-17 at 300 K (space group $P6_3/mmc$).

Table 4. Fractional Atomic Coordinates and Isotropic Temperature Factors for $AlPO_4$-17 at 18 and 300 K in Space Group $P6_3/mmc$

name	*x*	*y*	*z*	U_{iso} (Å^2)
		18 K		
T(1)	0.9982(2)	0.2366(1)	0.10181(8)	0.0098(3)
T(2)	0.3316(2)	0.4250(2)	0.2500	0.0098(3)
O(1)	0.0276(2)	0.3479(2)	0.1622(2)	0.0092(5)
O(2)	0.1003(2)	0.2008(4)	0.1139(3)	0.0092(5)
O(3)	−0.1269(2)	0.1269(2)	0.1282(3)	0.0092(5)
O(4)	0.0000	0.2746(2)	0.0000	0.0092(5)
O(5)	0.2287(3)	0.4574(5)	0.2500	0.0092(5)
O(6)	0.0846(5)	0.5423(2)	0.2500	0.0092(5)
		300 K		
T(1)	0.9984(2)	0.2370(1)	0.10108(8)	0.0130(3)
T(2)	0.3323(2)	0.4250(2)	0.2500	0.0130(3)
O(1)	0.0277(2)	0.3482(2)	0.1627(2)	0.0220(5)
O(2)	0.1007(2)	0.2015(4)	0.1122(3)	0.0220(5)
O(3)	−0.1269(2)	0.1269(2)	0.1272(3)	0.0220(5)
O(4)	0.0000	0.2758(3)	0.0000	0.0220(5)
O(5)	0.2287(3)	0.4574(5)	0.2500	0.0220(5)
O(6)	0.0840(5)	0.5420(3)	0.2500	0.0220(5)

Table 5. Selected Bond Distances (Å) and Angles (deg) in $AlPO_4$-17 at 300 K in Space Group $P6_3/mmc$

T(1)−O(1)	1.612(3)	2 × T(2)−O(1)	1.634(4)
T(1)−O(2)	1.631(2)	T(2)−O(5)	1.611(3)
T(1)−O(3)	1.601(2)	T(2)−O(6)	1.592(2)
T(1)−O(4)	1.627(1)		
mean T(1)−O	1.618	mean T(2)−O	1.618
O(1)−T(1)−O(2)	109.7(3)	O(1)−T(2)−O(1)	110.0(2)
O(1)−T(1)−O(3)	109.9(2)	2 × O(1)−T(2)−O(5)	109.2(2)
O(1)−T(1)−O(4)	108.4(2)	2 × O(1)−T(2)−O(6)	109.0(2)
O(2)−T(1)−O(3)	109.6(2)	O(5)−T(2)−O(6)	110.4(4)
O(2)−T(1)−O(4)	107.7(2)		
O(3)−T(1)−O(4)	111.5(2)		
T(1)−O(1)−T(2)	148.3(2)	T(1)−O(2)−T(1)	148.9(3)
T(1)−O(3)−T(1)	148.4(3)	T(1)−O(4)−T(1)	144.4(3)
T(2)−O(5)−T(2)	153.6(5)	T(2)−O(6)−T(2)	172.9(5)

The final observed, calculated, and difference plots for the structure at 300 K are shown in Figure 4.

Figure 5a−g shows the temperature dependence of the T−O bond distances, the internal O−T−O bond angles of the constituent tetrahedra, the bridging T−O−T angles, and the nearest neighbor nonbonding T−T distances within the structure. The internal bond angles of the constituent tetrahedra all lie within the range 107.6(2)° [O(2)−T(1)−O(4), 190 K] to 111.8(2)° [O(3)−T(1)−O(4), 190 K], with the largest difference between the maximum and minimum values found for a particular angle over the entire temperature range being 1.1° [O(5)−T(2)−O(6)] (Figure 5d,e). The bridging T−O−T angles all lie within the range 144.3(3)° [T(1)−O(4)−T(1), 250 K] to 173.4(5)° [T(2)−O(6)−T(2), 125 K], with the largest difference between the values found for a particular angle over the entire temperature range being 1.7° [T(2)−O(5)−T(2)] (Figure 5f). No significant changes over the temperature range analyzed were observed for either the internal O−T−O bond angles of the constituent tetrahedra or the bridging T−O−T angles.

The T−O bond distances are an average of the P−O (1.54 Å) and Al−O (1.74 Å) distances and all lie within the range 1.592(3) Å [T(2)−O(6), 300 K] to 1.648(4) Å [T(2)−O(1), 18 K], with the largest difference between the maximum and minimum values found for a particular T−O bond distance over the entire temperature range being 0.014 Å [T(2)−O(1)] (Figure 5b). There is an apparent decrease in the average T−O bond distance from 1.625 to 1.618 Å from 18 to 300 K (Figure 5c). However, both the Al−O and P−O bonds are strong, leading us to believe that the reduction in the average T−O bond distance is a result of correlated thermal motion in the solid.[20−22] After correcting for the thermal motion of the atoms,[23] the change in the average bond distance is 1.625−1.626 Å over the same range. This change (0.001 Å) in the average T−O bond distance is less than the average esd on a T−O bond distance (0.003 Å) and indicates that there is no detectable change in the average T−O bond length over this temperature range. The fact that the bond angles and corrected bond distances within the TO_4 tetrahedra remain essentially constant over the temperature range studied allows the latter to be considered as rigid tetrahedra.

Discussion

A possible explanation for thermal contraction in tetrahedral framework structures is a decrease in T−O−T angles with increasing temperature. In fact, some zeolites can expand and contract significantly by changing T−O−T angles with no significant change in T−O bond lengths.[24] Instead, our results shown in Figure 5f indicate that thermal contraction in $AlPO_4$-17 is not associated with decreasing T−O−T angles. Our results from the structure refinements of $AlPO_4$-17 in space group $P6_3/mmc$ lead us to believe that the negative thermal expansion of this material is related to the transverse vibrations of the 2-coordinate bridging oxygen atoms, a mode of lattice vibration that is of low enough energy to be readily excited at low temperatures. These vibrations lead to coupled rocking of the essentially rigid tetrahedra making up the structure of the material. The lack of any systematic changes in atomic coordinates and bond angles over the tempera-

(20) Cruickshank, D. W. J. *Acta Crystallogr.* **1956**, *9*, 757.
(21) Busing, W. R.; Levy, H. A. *Acta Crystallogr.* **1964**, *17*, 142.
(22) Willis, B. T. M.; Pryor, A. W. *Thermal Vibrations in Crystallography*; Cambridge University Press: Cambridge, UK, 1975.
(23) Downs, R. T.; Gibbs, C. V.; Bartelmehs, K. L.; Boisen, M. B., Jr. *Am. Miner.* **1992**, *77*, 754.
(24) Khosrovani, N.; Sleight, A. W. *J. Solid State Chem.* **1996**, *121*, 2.

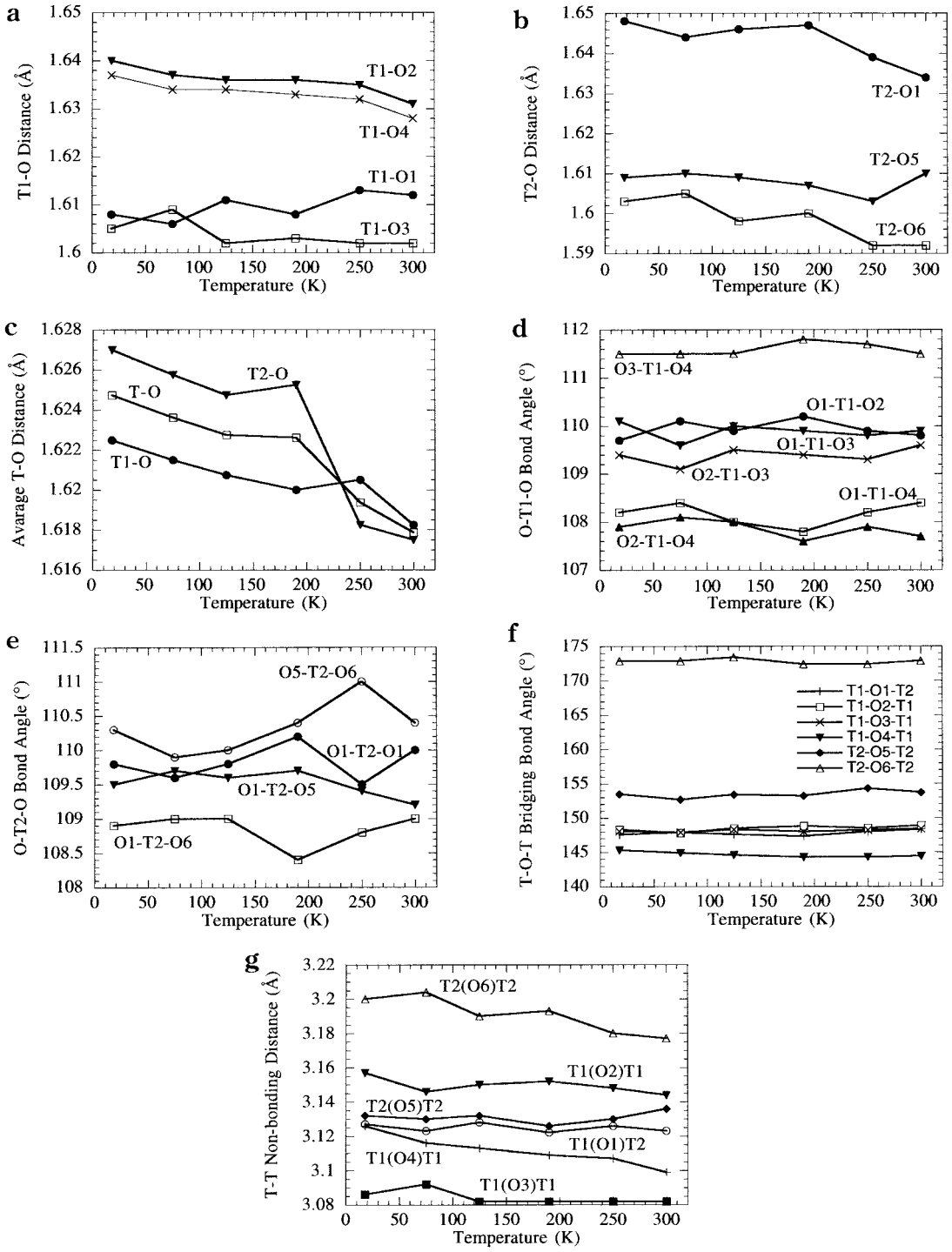

Figure 5. Selected bond distances and angles as a function of temperature: (a) T(1)−O bond distances, (b) T(2)−O bond distances, (c) average T−O bond distances, (d) O−T(1)−O internal tetrahedral bond angles, (e) O−T(2)−O internal tetrahedral bond angles; (f) T−O−T bridging bond angles, and (g) T−T nonbonding distances.

ture range studied implies that the transverse vibrations of the bridging oxygen atoms are essentially harmonic and the bending of the T−O−T bonds is dynamic rather than static in nature. As the temperature of the material is increased, the magnitude of the transverse vibrations of the bridging oxygen atoms, as well as the resulting coupled rotations of the tetrahedra, increases, which manifests itself in the structure refinement results as a decrease in the average T−O distance. With the decrease in the T−O bond length accompanying the increase in temperature, a decrease in the average T−T nonbonding distance occurs (Figure 5g), resulting in the negative thermal expansion observed. Again we emphasize that the apparent reduction of the T−O bond length results from the increased thermal motion and not from actual changes in the magnitude of the T−O vector. The explanation of the mechanism of negative thermal expansion for this aluminophosphate is the same as that suggested for other materials such as ZrW_2O_8[3,4,7] and siliceous faujasite.[6]

The theoretical prediction[13] for $AlPO_4$-17 was negative thermal expansion that was very temperature dependent, and this is not in agreement with our results. A value close to our observed value was calculated for a

temperature of 20 K, but a value of about -25×10^{-6} K^{-1} was calculated for the 100−300 K range.

The magnitude of the negative thermal expansion in $AlPO_4$-17 is approximately 3 times larger in the *a* and *b* direction than the *c* direction. Although this is difficult to fully explain, a factor that will contribute to this difference in magnitudes is the symmetry restrictions imposed on the structure, in both the $P6_3/m$ and $P6_3/mmc$ space groups. These restrictions only allow the tetrahedra of the 6-rings that link the cancrinite cages together to rotate about an axis parallel to the *c* direction. Because three [O(5)−T(2)−O(6)] of the five atoms in these tetrahedra lie in the *ab* plane, a much larger effect of the coupled rotations of the tetrahedra in these 6-rings will be exerted on the expansion behavior in the *ab* plane than in the *c* direction, resulting in the larger variation of the former.

The strong negative thermal expansion of $AlPO_4$-17 is the second example found in the family of zeolites and aluminophosphate materials. Other members are likely to exhibit such behavior. One possible empirical way that may be of use in predicting which members might contract upon heating is to compare the cell volume of the as-synthesized and the calcined dehydrated material. If the value of the former is less than the latter, the interaction of the framework with the template molecule is such as to cause the framework to contract around the template molecule. This shows that the particular framework has the ability to contract and may exhibit negative thermal expansion, as is seen to be the case for $AlPO_4$-17, where the cell volumes are 2241.4[17] and 2274.6 $Å^3$ for the as-synthesized and dehydrated calcined material at 300 K, respectively. Negative thermal expansion behavior has also been predicted for other members of the tetrahedral TO_2 family from computational methods.[9,13] However, the latter also predicts that some such framework materials exhibit positive thermal expansion. The reasons for the difference in behavior for similar materials remain unclear and are currently under investigation.

Acknowledgment. This work was supported through NSF grant DMR-9308530. Diffraction data were collected at the National Synchrotron Light Source, Brookhaven National Laboratory, which is supported by the U.S. Department of Energy, Division of Materials Sciences and Division of Chemical Sciences, under Contract No. DE-AC02-76CH00016.

CM9801587